High performance In_2O_3 nanowire transistors using organic gate nanodielectrics

Sanghyun Ju,[1] Fumiaki Ishikawa,[2] Pochiang Chen,[2] Hsiaokang Chang,[2] Chongwu Zhou,[2] Young-geun Ha,[3] Jun Liu,[3] Antonio Facchetti,[3] Tobin J. Marks,[3] and David B. Janes[4,a)]

[1]*Department of Physics, Kyonggi University, Suwon, Kyonggi-Do 442-760, Republic of Korea*
[2]*Department of Electrical Engineering, University of Southern California, Los Angeles, California 90089, USA*
[3]*Department of Chemistry and the Materials Research Center, and the Institute for Nanoelectronics and Computing, Northwestern University, Evanston, Illinois 60208-3113, USA*
[4]*School of Electrical and Computer Engineering, and Birck Nanotechnology Center, Purdue University, West Lafayette, Indiana 47907, USA*

(Received 20 December 2007; accepted 7 May 2008)

We report the fabrication of high performance nanowire transistors (NWTs) using In_2O_3 nanowires as the active channel and a self-assembled nanodielectric (SAND) as the gate insulator. The SAND-based single In_2O_3 NWTs are controlled by individually addressed gate electrodes. These devices exhibit *n*-type transistor characteristics with an on current of ~25 μA for a single In_2O_3 nanowire at $2.0V_{ds}$, $2.1V_{gs}$, a subthreshold slope of 0.2 V/decade, an on-off current ratio of 10^6, and a field-effect mobility of ~1450 cm^2/V s. These results demonstrate that SAND-based In_2O_3 NWTs are promising candidates for high performance nanoscale logic technologies. © *2008 American Institute of Physics*. [DOI: 10.1063/1.2937111]

Recently, there have been several studies of nanowire transistors (NWTs) aimed at achieving high performance and reliable transistor response characteristics. One potential application of NWTs is to replace polysilicon (poly-Si) or amorphous-silicon (α-Si) thin-film transistors (TFTs) currently used in displays, sensors, solar cells, and other optoelectronic devices.[1–4] NWTs have several attractions versus poly-Si TFTs and α-Si TFTs, in terms of high mobility, optical transparency (for large band-gap nanowires), and mechanical flexibility. These characteristics could allow higher frequency TFT operation and enable flexible/transparent electronics. For instance, future light-emitting diode-based displays could be integrated with optically transparent windows and/or operate at far lower power by enhancing the pixel aperture ratio. The latter parameter can be increased, for a given pixel spacing, by either stacking transparent TFT layers or significantly reducing the area required for the drive transistor. However, consideration of the NW-based device performance metrics reported to date reveals that there is significant room for improvement before NWT-derived driving and switching elements can be assembled into useful electronic circuits. Among several possible semiconducting nanowire materials, In_2O_3 is one of the most promising because of its easy access, chemical stability, and wide band gap (3.6 eV).[5–8] This combination of unique materials properties and the fundamental advantages of the quasi-one-dimensional nanowire electronic structure underscore the potential of In_2O_3 NWTs for advanced electronic applications requiring high transistor performance, optical transparency, and mechanical flexibility. In this study, we report significantly enhanced performance metrics for NWTs consisting of individual In_2O_3 nanowires as channels combined with a self-assembled organic nanodielectric[9] (SAND) as the gate insulator. The present SAND-based In_2O_3 NWTs demonstrate considerable advances in performance over previously reported NWTs employing In_2O_3 or other mid/wide bandgap NWTs, especially in terms of greatly improved field-effect mobility and high on-current densities.[10–16]

A cross-sectional view of the present NWT structure is shown in Fig. 1(a). Starting with a Corning 1737 glass substrate coated with a 500 nm SiO_2 buffer layer, individually addressable, transparent indium tin oxide (ITO) bottom-gate electrodes were deposited by ion-assisted deposition and photolithographically patterned. This individually addressable gate structure affords a high level of circuit integration

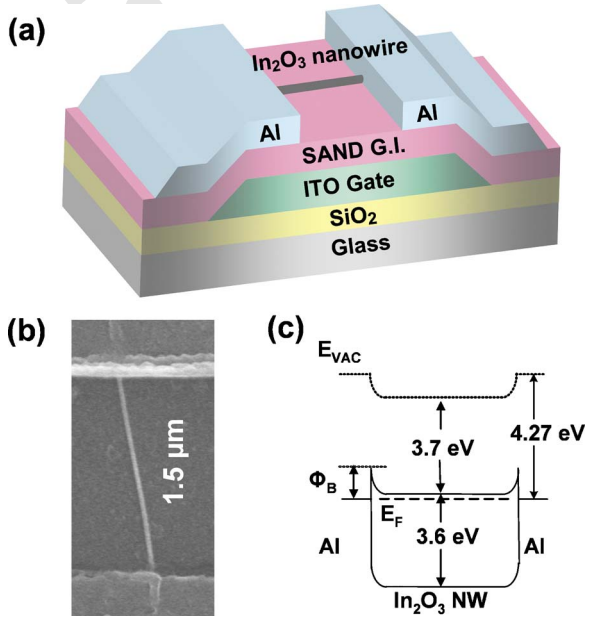

FIG. 1. (Color online) SAND-based In_2O_3 NWTs. (a) Cross-sectional view of the device structure. (b) Top-view FE-SEM images of the device region. Scale bar=1.5 μm. (c) Source/nanowire/drain cross-section band diagram at V_{gs}=0 V.

a)Author to whom correspondence should be addressed. Electronic addresses: janes@ccn.purdue.edu and david.b.janes.1@purdue.edu.

using NWTs. The SAND gate dielectric (~15 nm) was then deposited using a layer-by-layer wet chemical process and provides a large capacitance of ~180 nF/cm^2 with an electric breakdown field of ~7 MV/cm. The conformal SAND provides excellent edge coverage, resulting in low interlayer leakage in the gate and source-drain overlap regions. This high performance gate dielectric allows the channel potential to be modulated at relatively low gate voltages. The In_2O_3 nanowires, which were synthesized via laser ablation,[10] are not intentionally doped, but are believed to be lightly *n* type. The nanowires were suspended in isopropanol solution and then deposited onto the patterned substrates. Aluminum source/drain electrodes (~130 nm) were then deposited by electron-beam evaporation. Figure 1(b) shows a field-emission scanning electron (FE-SEM) micrograph of a single In_2O_3 nanowire confined between the source/drain electrodes. The diameter and length of the In_2O_3 nanowires are 20 nm and 1.5 μm, respectively. The corresponding band diagram (source/NW/drain cross section for an aluminum contact structure) for a NWT at V_{gs}=0 V is shown in Fig. 1(c). The electron affinity of In_2O_3 ($\chi_{In_2O_3}$) is 3.7 eV, and the bulk Fermi level position for moderate doping is estimated to be $(E_e\text{-}E_f)$=0.6 eV, yielding an effective work function $\Phi_{In_2O_3}$=4.54 eV for *n*-type material. Al source/drain contacts (Φ_{Al}=4.28 eV) are therefore expected to form relatively low interface barrier heights to *n*-type In_2O_3 NWs.

The present In_2O_3 NWTs exhibit excellent *n*-type transistor characteristics. All the NWT performance parameters reported here correspond to devices treated with ozone on the nanowire regions[17] with O_2 plasma polishing on the source-drain contact region to maximize device performance. Figure 2(a) shows the drain current versus gate-source voltage (I_{ds}-V_{gs}) characteristics for a representative single In_2O_3 NWT, on both linear and semilog scales, as well as the measured field-effect mobility inferred from the transconductance (g_m) at the respective gate voltage. The device exhibits a subthreshold slope (S) of 0.2 V/decade, an on-off current ratio (I_{on}/I_{off}) of 10^6, and a threshold voltage (V_{th}) of 0.0 V. The drain current versus drain-source voltage (I_{ds}-V_{ds}) characteristics of a representative NWT are shown in Fig. 2(b). These devices exhibit no evidence of saturation of the I_{ds} in the investigated potential bias range and exhibit an I_{on} ~25 μA for the single In_2O_3 nanowire at V_{ds}=2.0 V, V_{gs} =2.1 V, respectively. Although a possible mechanism for the nonideal I_{ds}-V_{ds} curve at high gate voltages might be ascribed to nanowire body leakage, in fact the measured leakage current through the SAND layer is only 30–40 pA at 4 V, indicating negligible leakage current through the gate dielectric. In order to allow direct comparison to other reported transistor performance data, including other NWTs, I_{on} can be expressed in terms of a current density of ~8 $\times 10^6$ A/cm^2, assuming uniform current flow throughout the nanowire cross section. The current per unit channel width is greater than 1 mA/μm, considering only the diameter of the nanowire. Importantly, this current level for a single nanowire is sufficient to drive a 176$\times$54 μm^2 size AMOLED pixel at 300 cd/m^2 in current-generation electroluminescent technologies.

The field-effect mobility is extracted from the measured g_m and the calculated gate-to-channel capacitance (C_i $=2\pi\varepsilon_0 k_{eff} L/\cosh^{-1}(1+t_{ox}/r)$) using $\mu=dI_{ds}/dV_{gs}\times L^2/C_i$ $\times 1/V_{ds}$, where the effective dielectric constant of SAND

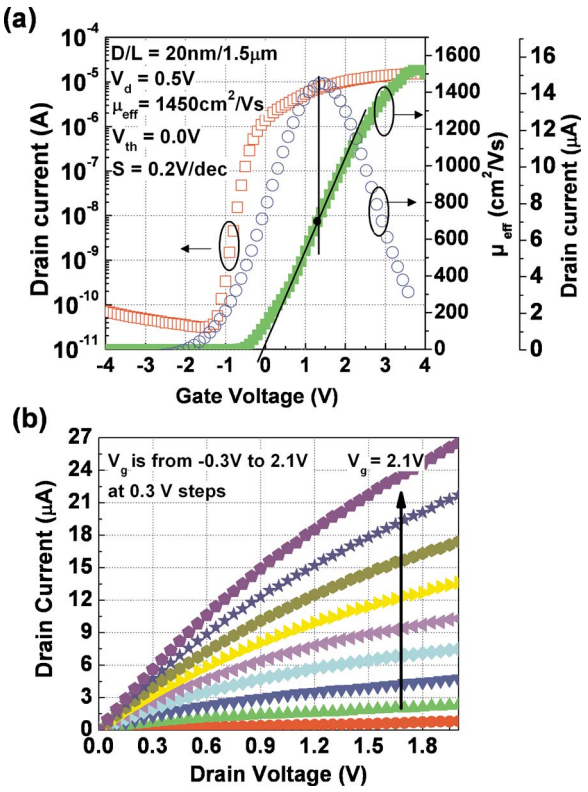

FIG. 2. (Color online) Measured characteristics of a representative SAND-based In_2O_3 NWT. (a) Drain current versus gate-source voltage (I_{ds}-V_{gs}) characteristics at V_d=0.5 V. Green, red, and blue data points correspond to linear-scale I_{ds}-V_{gs}, log-scale I_{ds}-V_{gs}, and and mobility μ. (b) Drain current vs drain-source voltage (I_{ds}-V_{ds}) characteristics for various values of V_{gs} (–0.3 to 2.1 V in 0.3 V steps).

(k_{eff}) is ~3.0, the device channel length (L) is ~1.5 μm, and the radius (r) of the In_2O_3 NW is 10 nm. The measured g_m at V_d=0.5 V, along with a Gaussian fit to the data, is illustrated in Fig. 3(a). The g_m peaks at ~5.87 μS, at V_g~1 V, and falls off with increasing gate voltage. The corresponding μ is plotted versus gate bias in Fig. 2(a) and varies from ~1450 cm^2/V s to ~300 cm^2/V s over the measured gate bias range. The peak mobility values of two other devices with from the same sample batch, with nominally identical structures, are ~1200 and 1170 cm^2/V s The peak value, which is typically quoted as the mobility in comparable devices, significantly exceeds In_2O_3 NW mobilities (μ =6.93–279 cm^2/V s) reported in other devices[10–13] and in single-crystal In_2O_3 (~160 cm^2/V s).[18] It is expected that the NW single-crystal nature along with the quasi-one-dimensional electronic structure, which inhibits low-angle scattering, contributes to the very large FET mobility. In addition, the SAND gate dielectric has previously been found to enable high performance in other oxide NWs.[19]

Several aspects of the observed current-voltage characteristics can be attributed to the effects of the contacts. While an ideal long-channel metal-oxide-semiconductor field-effect transistor (MOSFET) model describes the low V_{ds} data, the behavior at large V_{ds} deviates from the ideal MOSFET model both in terms of the nonsquare law relationship versus V_{gs} and the relatively large drain conductance. Based on calculated electrostatic screening lengths,[20] the characteristic length over which the bands bend at the metal-semiconductor (M-S) contact interface, as illustrated in Fig. 1(c), is estimated to be ~30 nm. This characteristic length

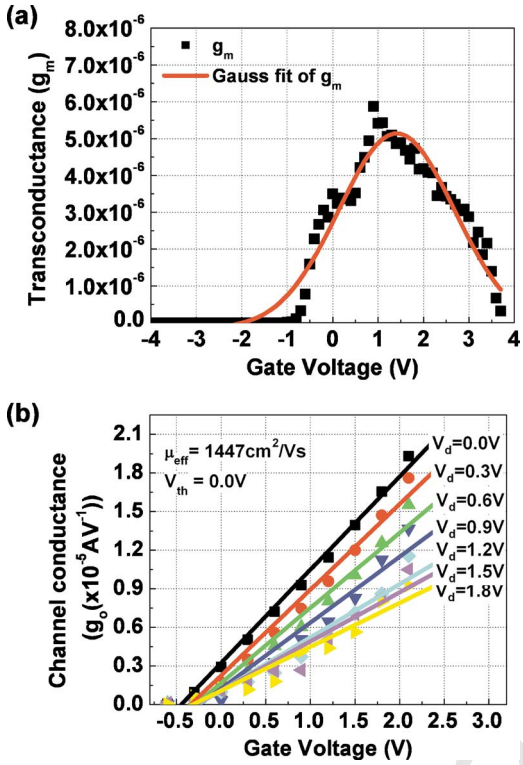

FIG. 3. (Color online) (a) Measured transconductance (g_m) at V_{ds}=0.5 V, along with a Gaussian fit to the data. (b) Measured channel conductance (g_d) vs V_{gs}, with various curves corresponding to steps in V_{ds} from 0.0 to 1.8 V.

would be reduced by channel charge induced by the gate potential or due to donor doping, which typically arises from oxygen vacancies in metal-oxide semiconductors. For this range of barrier thicknesses, it is expected that the contact behavior would be dominated by thermionic-field emission,[21] which would yield a nonlinear current-voltage characteristic for the M-S contacts. A prior study on NW transistors indicated that the effects of such a barrier in series with the channel included a roll-off in transconductance with increasing gate bias,[22] comparable to that observed in the present study. Figure 3(b) shows the measured channel conductance (g_d) versus gate voltage for various values of V_d. Linear series/contact resistance effects, would be expected to result in a saturation of g_d with increasing V_g.[23] However, no saturation is observed, indicating that linear series resistance effects are not dominant factors in the current-voltage (I-V) characteristics over the present bias range. The curves in Fig. 3(b) for low V_d values are somewhat superlinear, likely due to increasing conductance of the M-S contact barriers with increasing gate bias. These observations are consistent with the modest, but nonzero, M-S contact barrier illustrated in Fig. 1(c).

In conclusion, high performance, transparent NWTs have been fabricated using single In_2O_3 nanowires as the active channel, a SAND layer as the gate insulator, aluminum as source-drain electrodes, and ITO as the gate electrode. The single In_2O_3 NWTs were operated by individually addressable gate electrodes, which represents a significant advance toward circuit fabrication, and outstanding NWT device performance metrics were obtained using a SAND gate dielectric and proper processing of the In_2O_3 nanowire. As a result, we achieved significantly enhanced In_2O_3 NWT device performance and a significantly greater mobility than observed in poly-Si TFTs and α-Si TFTs. Since it is desirable to obtain high μ and a steep S to fabricate rapid-switching transistors and high-speed logic circuits, these results indicate that SAND-based In_2O_3 NWTs can support the requirements of such devices.

This work was supported in part by the NASA Institute for Nanoelectronics and Computing under Grant NCC-2-1363.

[1] J. Xiang, W. Lu, Y. Hu, Y. Wu, H. Yan, and C. M. Lieber, Nature (London) **441**, 489 (2006).
[2] Y. Cui, Z. Zhong, D. Wang, W. U. Wang, and C. M. Lieber, Nano Lett. **3**, 149 (2003).
[3] S. N. Cha, J. E. Jang, Y. Choi, G. W. Ho, D.-J. Kang, D. G. Hasko, M. E. Welland, and G. A. J. Amaratunga, Proceedings of the 38th European Solid-State Device Research Conference, 2005 (unpublished), Vol. 217.
[4] W. Kim, A. Javey, R. Tu, J. Cao, Q. Wang, and H. Dai, Appl. Phys. Lett. **87**, 173101 (2005).
[5] K. Sreenivas, T. S. Rao, and A. Mansingh, J. Appl. Phys. **57**, 384 (1985).
[6] Y. Shigesato, S. Takaki, and T. Haranoh, J. Appl. Phys. **71**, 3356 (1992).
[7] J. Tamaki, C. Naruo, Y. Yamamoto, and M. Mastuoka, Sens. Actuators B **83**, 190 (2002).
[8] M. Liess, Thin Solid Films **410**, 183 (2002).
[9] M.-H. Yoon, A. Facchetti, and T. J. Marks, Proc. Natl. Acad. Sci. U.S.A. **102**, 4678 (2005).
[10] C. Li, D. Zhang, S. Han, X. Liu, T. Tang, and C. Zhou, Adv. Mater. (Weinheim, Ger.) **15**, 143 (2003).
[11] B. Lei, C. Li, D. Zhang, T. Tang, and C. Zhou, Appl. Phys. A: Mater. Sci. Process. **79**, 439 (2004).
[12] D. Zhang, C. Li, S. Han, X. Liu, T. Tang, W. Jin, and C. Zhou, Appl. Phys. Lett. **82**, 112 (2003).
[13] N. Pho, H. T. Ng, T. Yamada, M. K. Smith, L. Jun, H. Jie, and M. Meyyappan, Nano Lett. **4**, 651 (2004).
[14] S. N. Cha, J. E. Jang, Y. Choi, G. A. J. Amaratunga, G. W. Ho, M. E. Welland, D. G. Hasko, D.-J. Kang, and J. M. Kim, Appl. Phys. Lett. **89**, 263102 (2006).
[15] T.-H. Moon, M.-C. Jeong, B.-Y. Oh, M.-H. Ham, M.-H. Jeun, W.-Y. Lee, and J.-M. Myung, Nanotechnology **17**, 2116 (2006).
[16] Y. W. Heo, L. C. Tien, Y. Kwon, D. P. Norton, S. J. Pearton, B. S. Kang, and F. Ren, Appl. Phys. Lett. **85**, 2274 (2004).
[17] S. Ju, K. Lee, D. B. Janes, M.-H. Yoon, A. Facchetti, and T. J. Marks, Nanotechnology **18**, 155201 (2007).
[18] R. L. Weiher, J. Appl. Phys. **33**, 2834 (1962).
[19] S. Ju, K. Lee, D. B. Janes, M.-H. Yoon, A. Facchetti, and T. J. Marks, Nano Lett. **5**, 2281 (2005).
[20] R.-H. Yan, A. Ourmazd, and K. F. Lee, IEEE Trans. Electron Devices **39**, 1704 (1992).
[21] F. A. Padovani and R. Stratton, Solid-State Electron. **9**, 695 (1966).
[22] J. Appenzeller, J. Knoch, E. Tutuc, M. Reuter, and S. Guha, Proceedings of 2006 Intl. Elect. Dev. Meeting (IEDM), IEEE, 2006 (unpublished), Vol. 1.
[23] Z. Yu and P. J. Burke, Proc. SPIE **5790**, 246 (2005).